AIP Advances

Amorphous molybdenum silicon superconducting thin films

D. Bosworth, S.-L. Sahonta, R. H. Hadfield, and Z. H. Barber

Citation: AIP Advances **5**, 087106 (2015); doi: 10.1063/1.4928285
View online: http://dx.doi.org/10.1063/1.4928285
View Table of Contents: http://scitation.aip.org/content/aip/journal/adva/5/8?ver=pdfcov
Published by the AIP Publishing

Articles you may be interested in

Coexistence of epitaxial Ta(111) and Ta(110) oriented magnetron sputtered thin film on c-cut sapphire
J. Vac. Sci. Technol. A **28**, 175 (2010); 10.1116/1.3276801

Enhanced superconducting transition temperature in FeSe 0.5 Te 0.5 thin films
Appl. Phys. Lett. **95**, 052504 (2009); 10.1063/1.3195076

Vortex matching effect in engineered thin films of NbN
Appl. Phys. Lett. **94**, 262501 (2009); 10.1063/1.3167771

Effect of implanted metal impurities on superconducting tungsten films
J. Appl. Phys. **91**, 6516 (2002); 10.1063/1.1469690

Continuous control of the superconducting transition temperature from overdoped to underdoped regimes in tetragonal Tl 2 Ba 2 CuO 6+δ thin films
Appl. Phys. Lett. **71**, 1706 (1997); 10.1063/1.120010

All article content, except where otherwise noted, is licensed under a Creative Commons Attribution 3.0 Unported license. See: http://creativecommons.org/licenses/by/3.0/ Downloaded to IP: 130.209.115.82 On: Tue, 18 Aug 2015 15:05:24

Amorphous molybdenum silicon superconducting thin films

D. Bosworth,[1,a] S.-L. Sahonta,[1] R. H. Hadfield,[2] and Z. H. Barber[1]
[1]*Department of Materials Science & Metallurgy, University of Cambridge, Cambridge CB3 0FS UK*
[2]*School of Engineering, University of Glasgow, Rankine Building, Oakfield Avenue, Glasgow G12 8LT, UK*

(Received 18 May 2015; accepted 28 July 2015; published online 4 August 2015)

Amorphous superconductors have become attractive candidate materials for superconducting nanowire single-photon detectors due to their ease of growth, homogeneity and competitive superconducting properties. To date the majority of devices have been fabricated using W_xSi_{1-x}, though other amorphous superconductors such as molybdenum silicide (Mo_xSi_{1-x}) offer increased transition temperature. This study focuses on the properties of MoSi thin films grown by magnetron sputtering. We examine how the composition and growth conditions affect film properties. For 100 nm film thickness, we report that the superconducting transition temperature (Tc) reaches a maximum of 7.6 K at a composition of $Mo_{83}Si_{17}$. The transition temperature and amorphous character can be improved by cooling of the substrate during growth which inhibits formation of a crystalline phase. X-ray diffraction and transmission electron microscopy studies confirm the absence of long range order. We observe that for a range of 6 common substrates (silicon, thermally oxidized silicon, R- and C-plane sapphire, x-plane lithium niobate and quartz), there is no variation in superconducting transition temperature, making MoSi an excellent candidate material for SNSPDs. © *2015 Author(s). All article content, except where otherwise noted, is licensed under a Creative Commons Attribution 3.0 Unported License.* [http://dx.doi.org/10.1063/1.4928285]

Amorphous superconductors were first studied in detail in the early 1980s[1–3] and as a result of their weak pinning centres and homogeneity[4] have been of interest in a range of fields including studies of vortex stability[5] and flux avalanches.[6]

Silicon- and germanium-based amorphous superconductors have attracted fresh interest due to their application in superconducting nanowire single photon detectors (SSPDs/SNSPDs).[7,8] These devices set new performance benchmarks for infrared photon counting,[9] offering low noise, record high count rates and improved spectral sensitivity compared to off-the-shelf photon counting technologies such as photomultipliers and semiconductor single photon avalanche photodiodes. Important infrared photon counting applications for SNSPDs include quantum communications,[10] ground-to-space communications,[11] quantum computing,[12] atmospheric remote sensing[13] and laser medicine.[14] While crystalline NbN and NbTiN are the most widely used materials for SNSPDs, amorphous superconductors offer various advantages,[15] including high uniformity, low superconducting gap energies (resulting in greater numbers of Cooper pairs being broken by an incident photon[16]), and lower critical currents (hence larger hotspots).[17] This all leads to more efficient detectors and extended long wavelength sensitivity.[18,19]

Amorphous W_xSi_{1-x} has been studied in some detail and shows performance comparable or exceeding that observed in Nb(Ti)N based SNSPD devices[20] with detection efficiencies of up to 40%,[15] and utilising optical stack architectures, efficiencies of up to 93% have been reported.[21] In

[a]Corresponding author: db412@cam.ac.uk

 ©Author(s) 2015

All article content, except where otherwise noted, is licensed under a Creative Commons Attribution 3.0 Unported license. See: http://creativecommons.org/licenses/by/3.0/ Downloaded to IP: 130.209.115.82 On: Tue, 18 Aug 2015 15:05:24

2014, Korneeva *et al* reported the first MoSi based SNSPD,[22] achieving 18% efficiency at 1200 nm wavelength. Very recently Verma *et al*[23] have reported cavity integrated SNSPDs, achieving up to 87 % efficiency at 1542 nm. This result approaches the efficiency of WSi devices at a higher operating temperature and with improved timing jitter. These studies emphasise the timeliness of understanding the behaviour and optimization of MoSi.

The motivation behind the use of amorphous superconductors for SNSPD applications is also based upon the potential for deposition of high quality films on unheated substrates. Crystalline superconductors such as NbN require high growth temperatures, exceeding 500 °C,[8] whereas, amorphous superconductors require low, ideally cryogenic, temperatures. These low deposition temperatures are more compatible with other components of integrated photonic circuits, for example III-V quantum dot devices[24] and ion implanted lithium niobate waveguides which are susceptible to damage on heating.[25] Studies of NbN SNSPD fabrication on GaAs[26] and lithium niobate[27] substrates highlight the considerable challenges of achieving high device yield on these materials platforms.

For amorphous transition metal alloys containing elements such as niobium, molybdenum and ruthenium, the transition temperature varies as a function of the number of valence electrons per atom (e/a), with the optimum e/a ratio being 6.4.[3] However these films must be grown at cryogenic temperatures to form amorphous structures and are susceptible to crystallisation upon warming to room temperature. A more stable alternative is to utilise metalloid materials such as silicon or germanium which promote and stabilise the formation of amorphous structures.[28] Mo_xSi_{1-x} has been shown to have a superconducting transition temperature (Tc) of around 7.3 K,[29] higher than the ≈6 K[30] observed for W_xSi_{1-x}.

This study aims to provide a more complete picture of the behaviour of MoSi thin films, exploring the variation of MoSi film properties with growth conditions, composition and thickness.

Amorphous films were deposited using DC magnetron sputtering on to a range of substrates. The films were deposited using a single alloy target (either $Mo_{80}Si_{20}$ or $Mo_{82}Si_{18}$) with, optionally, a pure (99.99%) Mo or Si target to enable fine-tuning of the composition. The substrates were placed on a rotatable substrate holder which could position the substrates in front of the alloy target for the entirety of the deposition, or sweep them alternately in front of the alloy target and an elemental target. By varying the power to each target, the composition can be controlled. In the latter case, a rotation frequency of 6 revolutions per minute was chosen to ensure complete mixing of the components. The copper substrate support (cylindrical, diameter 125 mm and thickness 65 mm) acts as a large thermal mass drawing heat away from the films during growth. Cooling was achieved by filling the hollow chamber walls with liquid nitrogen.

The chamber was evacuated to $<10^{-6}$ Pa before a dynamic equilibrium of 1.2 Pa of argon was achieved by balancing the argon in-flow with the pump rate. A power of 20 W was applied to the MoSi target, with between 5 and 20 W being applied to the Si or Mo target when used (all targets were 55 x 35 mm in area). The film thickness was controlled by varying the deposition time or the number of rotations of the substrates. Typically films were either 100 nm thick, a result of 5 minutes direct deposition or 60 rotations, or 5 nm thick, a result of 10 seconds or 2 rotations (the non-linearity for short depositions is due to the time taken for the substrate to move in and out of the depositing flux).

The superconducting transition temperature, Tc, was measured using a 4-point resistance probe which was dipped into liquid helium. The transition temperature is taken as the point where the resistance has fallen to half its value at 30 K while the transition width is the range between 10% and 90% of the 30 K resistance. Film composition was measured by using energy dispersive X-ray spectroscopy in a JEOL 5800 scanning electron microscope.

Film structure was characterized using X-ray diffraction (XRD) of 100 nm samples grown on single crystal silicon substrates. Plan view transmission electron microscopy (TEM) was performed using an FEI Osiris microscope operating at 200 kV. 5 nm thick MoSi samples were deposited directly onto holey carbon-coated TEM grids.

Three 100 nm thick films were grown under the same conditions on each of 6 substrate types, the resulting transition temperatures are shown in table I.

All article content, except where otherwise noted, is licensed under a Creative Commons Attribution 3.0 Unported license. See: http://creativecommons.org/licenses/by/3.0/ Downloaded to IP: 130.209.115.82 On: Tue, 18 Aug 2015 15:05:24

TABLE I. Superconducting transition temperature and transition width for 100 nm thick $Mo_{83}Si_{17}$ films grown on various substrates at approximately 0 °C.

Substrate	Tc (K)	ΔTc
Silicon (≈ 10 nm native oxide)	7.60 ± 0.15	0.05 ± 0.01
Silicon (150 nm thermally oxidized layer)	7.49 ± 0.10	0.07 ± 0.01
Quartz	7.53 ± 0.10	0.01 ± 0.01
X-plane Lithium Niobate	7.53 ± 0.15	0.03 ± 0.01
R-Plane Sapphire	7.41 ± 0.10	0.03 ± 0.01
C-Plane Sapphire	7.47 ± 0.10	0.005 ± 0.001

The variation between the samples is within the experimental error due to slight variation in deposition parameters, indicating that, as expected for amorphous superconductors, the choice of substrate material does not influence the transition temperature.

Cooled substrates are used to promote the formation of the amorphous phase; here we examine the effect of varying this cooling.

Prior to each sample being grown, a presputtering period of 15 minutes was used to stabilize the growth parameters. The first sample was deposited with no cooling and the substrate temperature rose during deposition to 62 °C. After an hour of cooling, sample 2 was deposited at 20 °C. Sample 3 was grown after a further hour of cooling and the substrate temperature reached 7.4 °C and sample 4 after a further 30 minutes resulting in a substrate temperature of -0.7 °C. Figure 1(a) shows the superconducting transition temperature and width for each film. Clearly, there is an increase in the transition temperature as the substrates are cooled.

The XRD traces in figure 1(b) illustrate that the sample grown without cooling contains significant crystallinity, as shown by the peak at around 41° (corresponding to the Mo_3Si (210) peak). However, once the substrate is cooled (below around 20 °C) the crystallinity drops significantly and no diffraction peak is visible. While all three samples grown with cooled substrates could be described as "X-ray amorphous", given that we see an increase in transition temperature as the substrates are cooled further, the lack of a diffraction peak is insufficient evidence for an optimised film structure. The stability of the amorphous phase as a function of temperature has been explored previously[31] although this study was limited to whether a film could be defined as amorphous or crystalline. Here we show that it is important to consider to what extent a film is amorphous.

Film structure was also characterised using TEM. Figure 2 shows images and diffraction patterns for samples grown without cooling, and after 3 hours of cooling.

Diffraction from the cooled specimen (figure 2(a)) results in multiple wide diffraction rings, with a high level of diffuse scattering intensity in between, characteristic of films with a high proportion of amorphous material. The uncooled specimen shows sharper diffraction rings with lower diffuse scattering intensity in between the rings, indicative of higher long-range order expected from a more crystalline film. The high-resolution images in figure 2(b) show short-range order in both specimens, indicated by the fact that some atomic columns are visible as speckled contrast throughout both structures. The Fourier transforms (figure 2(c)) show sharper spot periodicities for the uncooled specimen

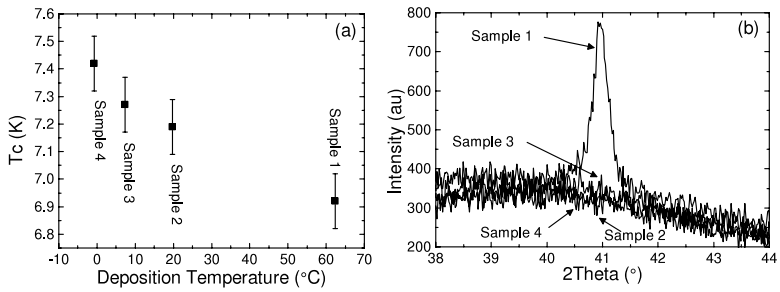

FIG. 1. *Data for 100 nm thick $Mo_{80}Si_{20}$ films on silicon substrates (a) Tc variation with deposition temperature (defined as the peak substrate temperature during film growth. (b) X-ray diffraction traces showing crystallinity of $Mo_{80}Si_{20}$ films.*

All article content, except where otherwise noted, is licensed under a Creative Commons Attribution 3.0 Unported license. See: http://creativecommons.org/licenses/by/3.0/ Downloaded to IP: 130.209.115.82 On: Tue, 18 Aug 2015 15:05:24

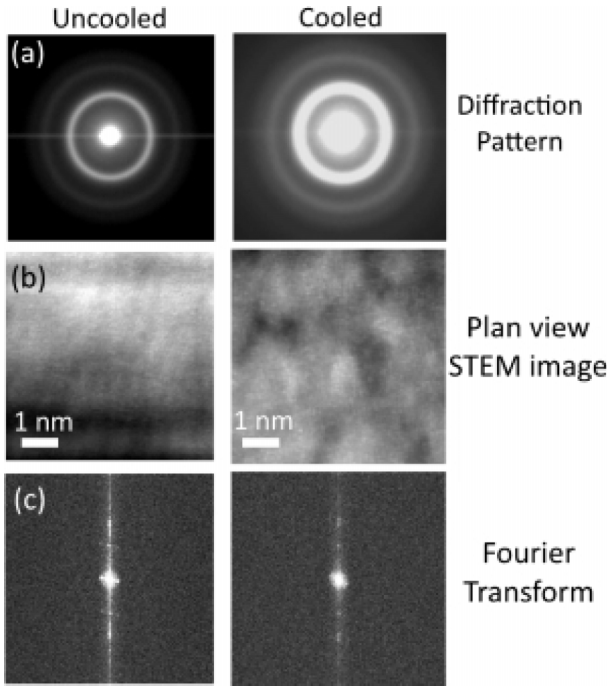

FIG. 2. *TEM data for two 5 nm thick $Mo_{80}Si_{20}$ samples grown on holey carbon copper TEM grids without cooling and with 3 hours of cooling. (a) Diffraction ring patterns, (b) high-resolution images (c) Fourier transforms of the images.*

than for the cooled specimen, suggesting that there is a more periodic atomic structure in the uncooled specimen. The TEM results alongside the XRD indicate that, while some short range order persists in all of the samples, long range order is significantly decreased for the cooled samples.

By varying the power to the secondary target (Mo or Si) it is possible to vary the film composition, which in turn has an effect on the transition temperature, as shown in figure 3.

There is a maximum in transition temperature for $Mo_{83}Si_{17}$ films. This is slightly different to the more widely used composition of $Mo_{80}Si_{20}$ although most composition studies[1,2,31] measured films over a much wider range and do not report such precise sample compositions. It is worth noting that our $Mo_{83}Si_{17}$ films were deposited by direct growth from a $Mo_{80}Si_{20}$, target, indicating non-ideal composition transfer to the film.

Collver and Hammond[3] measured the variation in Tc with the e/a ratio for a range of 4d and 5d metal alloys and found a maximum Tc for an e/a of 6.4. For ratios below this value, the transition temperature dropped at a rate of around 2.5 K for each valence electron lost, however the trend seen

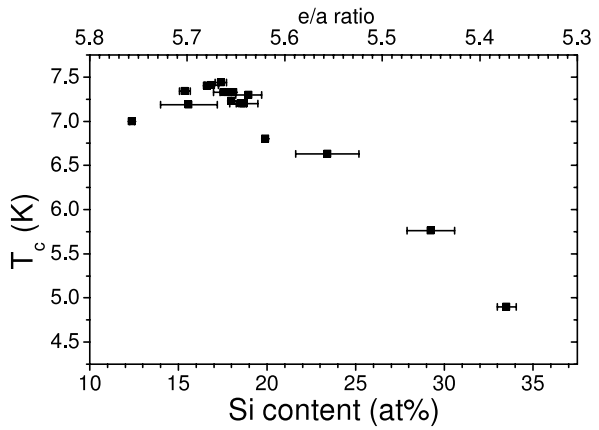

FIG. 3. *Transition temperature of 100 nm thick films grown on cooled silicon substrates as a function of composition.*

All article content, except where otherwise noted, is licensed under a Creative Commons Attribution 3.0 Unported license. See: http://creativecommons.org/licenses/by/3.0/ Downloaded to IP: 130.209.115.82 On: Tue, 18 Aug 2015 15:05:24

here is much steeper. The role of silicon is not simply as a valence electron source, indeed Edelstein *et al*[1] raise concern over interpreting silicon in such a way, since it is not a transition metal. They found it possible to fit a reasonable model to the data if silicon is taken to contribute 4 electrons which would suggest an optimum e/a value of 5.66 rather than the 6.4 found for metal-metal alloys, with the transition temperature dropping off sharply for compositions greater than 17 % silicon.

The decrease in Tc as the silicon content falls below the optimum value is attributed to an increased amount of crystalline material forming.[2] The stability of the amorphous phase is a function of composition and temperature. As the silicon content decreases, the Tc is observed to increase until there is insufficient silicon to promote the formation of the amorphous phase, at which point the crystalline phase begins to compromise the superconducting properties. Given that the formation of the crystalline phase is inhibited by low deposition temperatures, it is likely that the optimum composition is itself a function of growth temperature. Extrapolating our high silicon content Tc data to zero silicon case is consistent with the reported Tc for amorphous pure Mo of around 8 K,[32] though amorphous Mo is not stable at room temperature,[3] transforming to a body centred cubic structure with a Tc of around 1 K.[31] In summary, by reducing the growth temperature, it is possible to grow amorphous films with lower silicon contents which, in turn, have superior superconducting properties; but this may reduce the stability of the amorphous phase.

Figure 4 shows the reduction in transition temperature as film thickness is reduced which is of great importance for SNSPD applications.

The decrease in transition temperature with thickness is a well known phenomenon[33] although the mechanism is still unclear. The behaviour can be partially modelled using proximity effect and quantum size effect theories[34,35] which argue that the transition temperature varies with thickness directly, however an alternative analysis shows that there is a correlation between transition temperature and resistivity[36] which has some theoretical explanation.[37] Resistivity is shown as a function of film thickness in figure 4.

The complication in explaining the change in transition temperature comes from two related effects. Firstly, there are the localisation and interaction effects which become more significant for thin films, however the presence of defects or other inhomogeneities will also become more significant. It is therefore difficult to determine whether the film quality itself is lower for thin films, or if the decreased transition temperature is a fundamental effect of the reduced dimensions. If the former, then improvements can be made to the film growth in order to limit the degradation of properties. Korneeva *et al*[22] have used a silicon capping layer to reduce damage to the film during processing and to prevent oxidation.

Thin film amorphous MoSi superconductor is an attractive material for various fundamental studies and for applications in SNSPDs. Our study shows that tuning the silicon content promotes the formation of the amorphous phase and allows for an optimum superconducting transition temperature to be achieved. Moreover we show that by decreasing the substrate temperature during growth (from 63 °C to 0 °C), the formation of the amorphous phase can be promoted which, in turn, results in a

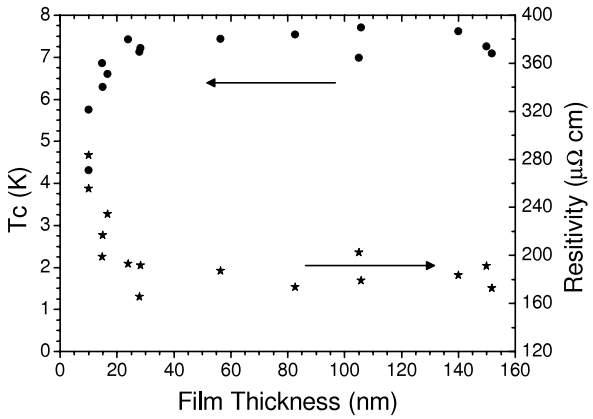

FIG. 4. *Variation in Tc and resistivity with film thickness for $Mo_{83}Si_{17}$ films grown on cooled silicon substrates.*

All article content, except where otherwise noted, is licensed under a Creative Commons Attribution 3.0 Unported license. See: http://creativecommons.org/licenses/by/3.0/ Downloaded to IP: 130.209.115.82 On: Tue, 18 Aug 2015 15:05:24

higher transition temperature (7.4 K for 100 nm film thickness). Control of the silicon content is then vital to ensure that the amorphous phase remains stable at room temperature; too little silicon and the films will crystallise, too much and there is a detrimental effect on the superconducting properties. Due to the amorphous nature of the films, the choice of substrate material is not critical, which is a significant result for flexible optimisation of high performance SNSPDs within advanced optical devices architectures, such as optical cavities and photonic integrated circuits.

This work was supported by the EPSRC through grant EP/I036303/1. RHH acknowledges a Royal Society of London University Research Fellowship. The data used in this paper can be accessed at https://www.repository.cam.ac.uk/handle/1810/247704

[1] A. Edelstein and S. Ovshinsky, Solid State Commun. **41**, 139 (1982).
[2] M. Ikebe, Y. Muto, S. Ikeda, H. Fujimori, and K. Suzuki, Phys. B+ C **107**, 387 (1981).
[3] M. Collver and R. Hammond, Phys. Rev. Lett. **30**, 92 (1973).
[4] H.T. Huy, H. Shishido, M. Hayashi, T. Yotsuya, M. Kato, and T. Ishida, Phys. C Supercond. **484**, 86 (2013).
[5] M. Liang and M.N. Kunchur, Phys. Rev. B **82**, 144517 (2010).
[6] F. Colauto, M. Motta, and A. Palau, arXiv:1408.4650v1 (2014).
[7] C.M. Natarajan, M.G. Tanner, and R.H. Hadfield, Supercond. Sci. Technol. **25**, 063001 (2012).
[8] G.N. Gol'tsman, O. Okunev, G. Chulkova, a. Lipatov, a. Semenov, K. Smirnov, B. Voronov, a. Dzardanov, C. Williams, and R. Sobolewski, Appl. Phys. Lett. **79**, 705 (2001).
[9] R.H. Hadfield, Nat. Photonics **3**, 696 (2009).
[10] H. Takesue, S.W. Nam, Q. Zhang, R.H. Hadfield, T. Honjo, K. Tamaki, and Y. Yamamoto, Nat. Photonics **1**, 343 (2007).
[11] M.E. Grein, A.J. Kerman, E. a. Dauler, O. Shatrovoy, R.J. Molnar, D. Rosenberg, J. Yoon, C.E. Devoe, D. V. Murphy, B.S. Robinson, and D.M. Boroson, in *Int. Conf. Sp. Opt. Syst. Appl. ICSOS'11* (2011) p. 78.
[12] D. Bonneau, M. Lobino, P. Jiang, C.M. Natarajan, M.G. Tanner, R.H. Hadfield, S.N. Dorenbos, V. Zwiller, M.G. Thompson, and J.L. O'Brien, Phys. Rev. Lett. **108**, 1 (2012).
[13] A. McCarthy, N.J. Krichel, N.R. Gemmell, X. Ren, M.G. Tanner, S.N. Dorenbos, V. Zwiller, R.H. Hadfield, and G.S. Buller, Opt. Express **21**, 8904 (2013).
[14] N.R. Gemmell, A. McCarthy, B. Liu, M.G. Tanner, S.D. Dorenbos, V. Zwiller, M.S. Patterson, G.S. Buller, B.C. Wilson, and R.H. Hadfield, Opt. Express **21**, 5005 (2013).
[15] B. Baek, A.E. Lita, V. Verma, and S.W. Nam, Appl. Phys. Lett. **98**, 251105 (2011).
[16] V.B. Verma, a. E. Lita, M.R. Vissers, F. Marsili, D.P. Pappas, R.P. Mirin, and S.W. Nam, Appl. Phys. Lett. **105**, 022602 (2014).
[17] B. Baek, A.E. Lita, V. Verma, and S.W. Nam, Appl. Phys. Lett. **98**, 251105 (2011).
[18] F. Marsili, F. Bellei, F. Najafi, A. Dane, E. a Dauler, R.J. Molnar, and K. Berggren, Nano Lett. **12**, 4799 (2012).
[19] a. Engel, a. Aeschbacher, K. Inderbitzin, a. Schilling, K. Il'In, M. Hofherr, M. Siegel, a. Semenov, and H.W. Hübers, Appl. Phys. Lett. **100**, 10 (2012).
[20] S.N. Dorenbos, P. Forn-Díaz, T. Fuse, a. H. Verbruggen, T. Zijlstra, T.M. Klapwijk, and V. Zwiller, Appl. Phys. Lett. **98**, 251102 (2011).
[21] F. Marsili, V. Verma, J. Stern, and S. Harrington, Nat. Photonics **7**, 210 (2013).
[22] Y.P. Korneeva, M.Y. Mikhailov, Y.P. Pershin, N.N. Manova, a V Divochiy, Y.B. Vakhtomin, a a Korneev, K. V Smirnov, a G. Sivakov, a Y. Devizenko, and G.N. Goltsman, Supercond. Sci. Technol. **27**, 095012 (2014).
[23] V.B. Verma, B. Korzh, F. Bussières, R.D. Horansky, S.D. Dyer, A.E. Lita, I. Vayshenker, F. Marsili, M.D. Shaw, H. Zbinden, R.P. Mirin, and S.W. Nam, arXiv, (2015).
[24] G. Reithmaier, S. Lichtmannecker, T. Reichert, P. Hasch, K. Müller, M. Bichler, R. Gross, and J.J. Finley, Sci. Rep. **3**, 1901 (2013).
[25] R. Osellame, M. Lobino, N. Chiodo, M. Marangoni, G. Cerullo, R. Ramponi, H.T. Bookey, R.R. Thomson, N.D. Psaila, and A.K. Kar, Appl. Phys. Lett. **90**, 241107 (2007).
[26] a. Gaggero, S.J. Nejad, F. Marsili, F. Mattioli, R. Leoni, D. Bitauld, D. Sahin, G.J. Hamhuis, R. Nötzel, R. Sanjines, and a. Fiore, Appl. Phys. Lett. **97**, 97 (2010).
[27] M.G. Tanner, L.S.E. Alvarez, W. Jiang, R.J. Warburton, Z.H. Barber, and R.H. Hadfield, Nanotechnology **23**, 505201 (2012).
[28] W.L. Johnson, J. Appl. Phys. **50**, 1557 (1979).
[29] S. Kubo, J. Appl. Phys. **63**, 2033 (1988).
[30] S. Kondo, J. Mater. Res. **7**, 853 (1992).
[31] W.L. Johnson, C.C. Tsuei, S.I. Raider, and R.B. Laibowitz, J. Appl. Phys. **50**, 4240 (1979).
[32] R. Koepke and G. Bergmann, Solid State Commun. **19**, 435 (1976).
[33] M. Strongin, R. Thompson, O. Kammerer, and J. Crow, Phys. Rev. B **1**, 1078 (1970).
[34] Y. Liu, D.B. Haviland, B. Nease, and a. M. Goldman, Phys. Rev. B **47**, 5931 (1993).
[35] H.M. Jaeger, D.B. Haviland, B.G. Orr, and a. M. Goldman, Phys. Rev. B **40**, 182 (1989).
[36] Y. Ivry, C.-S. Kim, a. E. Dane, D. De Fazio, a. N. McCaughan, K. a. Sunter, Q. Zhao, and K.K. Berggren, Phys. Rev. B **90**, 214515 (2014).
[37] M. Beasley, J. Mooij, and T. Orlando, Phys. Rev. Lett. **42**, 1165 (1979).

All article content, except where otherwise noted, is licensed under a Creative Commons Attribution 3.0 Unported license. See: http://creativecommons.org/licenses/by/3.0/ Downloaded to IP: 130.209.115.82 On: Tue, 18 Aug 2015 15:05:24